Surface magnetism; magnetization and anisotropy at a surface

1991 J. Phys.: Condens. Matter 3 4497

(http://iopscience.iop.org/0953-8984/3/25/001)

J. Phys.: Condens. Matter 3 (1991) 4497–4522. Printed in the UK

REVIEW ARTICLE

Surface magnetism; magnetization and anisotropy at a surface

T Kaneyoshi
Department of Physics, Nagoya University, 464-01 Nagoya, Japan

Received 20 February 1991

Abstract. A review is given of surface magnetism. In particular the interplay of magnetization and anisotropy at a surface is discussed, after a survey of experimental and theoretical results for magnetic moment and anisotropy at surfaces or interfaces of semi-infinite magnets and thin films. Finally, the importance for surface (or interface) analysis of the random single-ion anisotropy model is stressed.

1. Introduction

Magnetic behaviour near a surface (or an interface) in a magnetically ordered solid may differ in many respects from that inside. This is due to the fact that the reduced symmetry, lower coordination number, and the availability and role of highly localized surface and interface states offer the possibility of inducing new magnetic structures with new and interesting magnetic phenomena. These phenomena may occur locally at, or only a few atomic layers below, the surface (or interface). The study of these phenomena belongs to the field of surface magnetism in its strictest meaning. The existence of a surface can also affect the magnetic properties in the interior of the material, such as magnetic domain structure and spin arrangements. Such disturbances extend from the surface into the interior to depths ranging from a few tens to several thousands of ångstroms or more.

The surface magnetic properties of semi-infinite magnetic systems (or the surface magnetism) have been extensively studied for many years by the use of a variety of experimental and theoretical techniques. In particular, they have been examined theoretically on the basis of a localized spin model, namely the semi-infinite spin-$\frac{1}{2}$ Ising model with various free surfaces.

The effects of surfaces on phase transitions have received much attention. In the early stages of these investigations Mills [1] assumed a model in which the spins in the free surface interact with one another with an exchange parameter J_s which is different from the bulk exchange J. The system is chosen as the semi-infinite simple cubic spin-$\frac{1}{2}$ Ising ferromagnet with the (100) free surface. For this simple model with modified exchange only at the surface, it was pointed out that, on the basis of the traditional mean-field approximation (MFA), for J_s greater than a critical value J_{sc} the system would order on the surface before it ordered in the bulk. Since then, a number of authors have investigated the possibility of this surface magnetic phase. This MFA prediction is now confirmed to be qualitatively correct. This model, in addition to its

0953-8984/91/254497+26$03.50

variations, is called a prototype of surface magnetism. Experimentally, the interesting phenomenon of surface enhanced magnetic order, i.e. the coexistence of an ordered surface with a disordered bulk, has been observed in two of the 4f rare-earth metals: gadolinium and terbium. For various studies of the prototype, see the review articles [2–4]. Most of these works, however, do not take into account the effects of spin-wave excitations at the surfaces of semi-infinite magnets, about which one should consult the review works [5–8]. For research on surface magnetism based on an itinerant electron model of transition-metal surfaces and interfaces, see the reviews reported in [9–10].

On the other hand, recent experiments show that there exists a very strong anisotropy field acting on spins in the surface or at the interface. This surface anisotropy is due to various causes associated with the material and its structure as well as the presence of the surface itself. In particular, recent experiments on magnetic films, epitaxially grown on non-magnetic substrates from a monolayer to several thousand layers, clearly exhibit the existence of surface anisotropy. The role of surface anisotropy has been proved to be of paramount importance in determining the magnetic properties of surfaces and thin films.

It is the aim of this article to review the present state of surface magnetism, especially paying attention to the influences of surface anisotropy on magnetic properties. The contents of this work are as follows.

Section 2 Some aspects of surface magnetism: 2.1, magnetic moment at the surface; 2.2, surface anisotropy; 2.3, surface-induced magnetic structure.

Section 3 Prototype of surface magnetism: 3.1, phase diagram; 3.2, surface magnetization curve.

Section 4 The effects of surface single-ion anisotropy: 4.1, surface tricritical behaviours; 4.2, relation to experimental results (I); 4.3, relation to experimental results (II); 4.4, critical phenomena; 4.5, related works.

Section 5 Random anisotropy at the surface or interface.

2. Some aspects of surface magnetism

2.1. Magnetic moment at the surface

First of all, the local magnetic moment of a surface atom at $T = 0$ K must be made clear. In the case of a transition-metal surface, it depends on the local environment. Theoretically, the magnetic moment at the surface can be determined by taking account of many factors; the surface shifts of the electronic states, intra-atomic s–d charge transfer, change in the s–d hybridization and the band-narrowing due to the reduction of the coordination number. Experimentally, it depends sensitively on the quality of sample preparation and the measuring method. Table 1 summarizes the calculated magnetic moments for the surface atoms, solving the local spin density functional equations self-consistently with the use of the full-potential linearized augmented plane wave method [11, 12]. In the table, the bulk counterparts are also given for comparison. In each case, the magnetic moment at the surface is larger than that of the bulk. In the simplest view, for instance, surface iron atoms interpolate between the properties of bulk atoms and free atoms.

On the other hand, the surface magnetic moments of semi-infinite rare-earth systems are not yet clarified. For example, Gd is a nearly isotropic ferromagnetic metal with a saturation magnetization of 7.55 μ_B per atom where 7 μ_B are attributed to the

Table 1. Calculated magnetic moments (in μ_B) for 3d transition metals [12].

		V	Cr	Fe	Ni	BCC-Co
Surface	(100)	0	2.49	2.98	0.68	1.95
	(110)			2.63	0.63	1.84
Bulk		0	0.59	2.25	0.56	1.76

seven localized electrons in the half-filled 4f shell and 0.55 μ_B are due to the polarization of the 5d–6s conduction electrons. But the magnetic moment of the ferromagnetic Gd(001) monolayer has very recently been shown to be 7.89 μ_B, primarily due to the increase of the 5d electron magnetic moment [13]. This enhancement agrees with that found for the transition-metal surfaces. The same situation may be expected for the surfaces of semi-infinite rare-earth systems.

In particular, recent experimental and theoretical work on a magnetic monolayer on a non-magnetic or paramagnetic substrate reveals the existence of a live magnetic (or a finite magnetic moment) surface plane (for example, see [13, 14]). Thus, these results clearly show that the concept of a dead surface layer (or no magnetic moment at a surface) [15] is not generally believed, although the term, dead layer, is often used.

2.2. Surface anisotropy

In addition to the existence of a finite magnetic moment at a surface atom, the direction of the moment is of interest. Each spin at the topmost layer of a semi-infinite magnet has a lower symmetry than that in the bulk. The lower symmetry at the surface produces an additional lower symmetry surface anisotropy term, which in many cases can be larger than the bulk. This fact was first treated by Néel [16] based on a phenomenological approach, and the magnetocrystalline anisotropy arises from an interplay between the spin–orbit coupling and the local crystalline electric field. For a high symmetry surface, that is (001), the surface anisotropy is given by a surface energy density,

$$E_s = K_s \cos^2 \theta \tag{1}$$

where K_s is the surface anisotropy constant and θ is the angle between the spontaneous magnetization M_s and the normal to the surface [17]. When K_s is negative, the energy is minimized for $\theta = 0$ corresponding to perpendicular magnetization and when $K_s > 0$ the energy is minimized for $\theta = \frac{1}{2}\pi$ or in-plane magnetization.

Besides the anisotropy energy, there exists a shape anisotropy at a surface due to various contributions; the demagnetizing field of the ordinary magnetic dipole–dipole interaction and the surface features, such as surface irregularities. The value of the shape anisotropy depends on the surface treatment as well as the shape of the sample.

In a ferromagnetic thin film, there generally exists a perpendicular uniaxial anisotropy ($K_s < 0$) resulting from the reduced symmetry at the surface. But the magnetization is usually oriented parallel to the surface plane due to the shape anisotropy. If the perpendicular anisotropy is large enough, it can overcome the shape anisotropy and force the magnetization to be perpendicular to the plane of the film. In extremely thin films, the magnetization may be oriented normal to the film plane, since the shape anisotropy decreases with a decrease in thickness. In fact, recent experiments [18–20]

show that there is an easy axis normal to the surface for spins in the surface of single crystal Fe or ultrathin Fe films. The effective surface anisotropy field can be inferred to be in the range of 50–100 kG in such samples. Other measurements [21–25] also suggest the possibility of large surface anisotropies.

Theoretically, the source of magnetocrystalline anisotropy in a ferromagnet has been considered to be due to the spin–orbit interaction. However, the anisotropy is a sensitive function of details of the electronic structure and hence the accurate surface electronic structure is required for the evaluation of surface anisotropy. A recent calculation [26] for a single layer of Fe(100) indicates a surface anisotropy K_s that is negative and approximately 100 times that of the bulk. On the other hand, other works [27, 28] predict different easy axes for an Fe(100) monolayer in contrast with the work [26], although much larger anisotropy energies than those of bulk energies are predicted for free-standing monolayers of transition-metal elements. In order to compare these values with experiment, the interaction of the monolayer with the substrate must be taken into consideration [29].

For Gd(0001) films on a W(110) substrate, the surface magnetic anisotropy is measured by changing the film thickness in the ferromagnetic phase from 1300 Å down to 0.8 monolayer [30]. For instance, the magnetic anisotropy energies of the 130 and 1300 Å films at a low temperature ($T/T_c = 0.38$) are enhanced by a factor of ten and two respectively, compared with bulk Gd. The first- and second-order contributions K_2 and K_4 to the uniaxial anisotropy are also determined. In figure 1, the temperature dependences of the effective uniaxial anisotropy constant $K_{eff}(T)[K_{eff}(T) = K_2(T) + K_4(T)]$ for three different Gd(0001) films are plotted as a function of temperature. However, the easy direction of the magnetization of Gd films is found to lie in the surface plane for all temperatures measured. The reason is due to the demagnetization energy which dominates the intrinsic magnetocrystalline effects. But, the temperature dependence of the 130 Å film indicates that at very low temperatures ($\simeq$ 20 K) the uniaxial anisotropy may overcome the demagnetizing energy and the easy direction may switch to the normal direction.

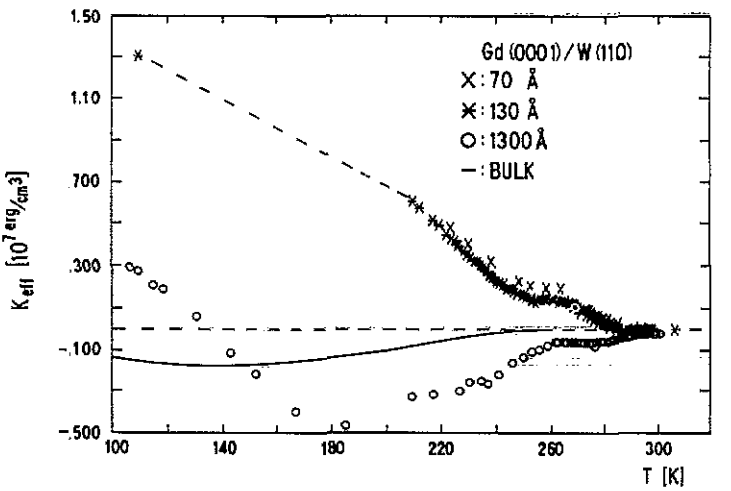

Figure 1. The thermal variations of the effective uniaxial anisotropy energy $K_{eff}(T)$ for three different Gd(0001) films on W(110) of thickness (70, 130 and 1300 Å). The full curve denotes the bulk $K_{eff}(T)$. The DC-field is applied in the film plane for these measurements [30].

2.3. Surface-induced magnetic structure

The Mössbauer experiment with Fe(110) films on a W(110) substrate [31] indicates that the surface magnetization M_s lies in the film plane and is along [110], in contrast to the bulk easy axis [001]. In general, the spins on a layer do not suddenly change their direction on the next layer: The Mössbauer result means that the rotation of the direction of spins on each layer parallel to the surface occurs in a certain region near the surface. In other words, surface-induced domain walls exist in the region [4].

Recent experiments [32, 33] clearly show that at the surface a bulk Bloch wall may change into a Néel wall in order to reduce the magnetic stray field energy of the ferromagnetic system. It is found on Fe(110) that, in spite of the dramatic change in the wall structure, the wall width at the surface is about the same as that inside the sample [32]; a width of (210 ± 40) nm is obtained for the 180° Bloch walls. The experiment [33] on magnetization orientations in domain walls at the surfaces of some magnetic materials, namely an Fe crystal, a ferromagnetic glass and a permalloy film, shows surface Néel wall profiles which are at least twice as wide as interior Bloch walls in bulk. See also [34].

3. Prototype for surface magnetism

As noted in section 2, recent experiments show that there exists a very strong anisotropy field acting on the spins in the surface or at the interface. This surface anisotropy is due to various causes associated with the material and its structure, as well as the presence of the surface itself. The role of surface anisotropy is proving to be of paramount important in determining the magnetic properties of surface and thin films. Before discussing the effects of surface anisotropy on magnetic properties, let us first review some essential points of phase diagrams and layered magnetizations for the prototype.

The magnetic behaviour of a semi-infinite simple cubic spin-$\frac{1}{2}$ Ising model with a (100) free surface (or the prototype of surface magnetism) has been extensively investigated for many years. In particular, the surface effects on phase transition have received much attention and have been studied using a variety of approximations and mathematical techniques. Figure 2 shows schematically a two-dimensional cross section through a semi-infinite simple cubic lattice with the (100) free surface. The Hamiltonian of the prototype is given by

$$H = -\sum_{(ij)} J_{ij} S_i^z S_j^z \tag{2}$$

where S_i^z takes the values ± 1 and the summation is carried out only over nearest-neighbour pairs of spins. J_{ij} is the exchange interaction with $J_{ij} = J_s$ if both i and j sites belong to the (100) surface and $J_{ij} = J$ otherwise.

For the spin-$\frac{1}{2}$ Ising model, one can easily prove that the expectation value of the spin variable S_i^z at a site i is represented by an exact identity [34]:

$$\langle S_i^z \rangle = \langle \tanh(\beta E_i) \rangle \tag{3}$$

with

$$E = \sum_j J_{ij} S_j^z \tag{4}$$

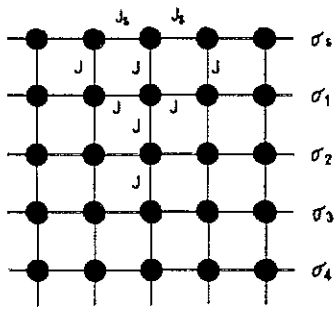

Figure 2. Part of a two-dimensional cross section through the semi-infinite simple cubic Ising lattice with a free surface. Full circles denote lattice points which are occupied by spins $S_i^z = \pm 1$.

where $\beta = 1/k_B T$. Here, the traditional MFA can be obtained from (3) by approximating the thermal average of the hyperbolic tangent with the hyperbolic tangent of the thermal average, that is

$$\langle \tanh(\beta E_i) \rangle \simeq \tanh(\beta \langle E_i \rangle) \tag{5}$$

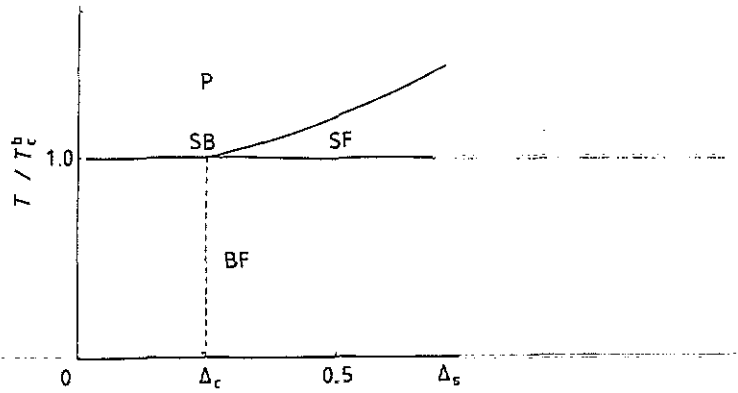

Figure 3. Phase diagram in the (T, Δ_s) space for the simple cubic Ising model with a free surface and enhanced surface coupling (6).

3.1. Phase diagram

The presence of the surface may modify the interaction in the surface layer, which is normally given by

$$J_s = J(1 + \Delta_s) \tag{6}$$

that is, the surface exchange interaction J_s is often scaled with that of bulk in the prototype of the surface magnetism. Figure 3 shows a phase diagram generally expected for the prototype; if the parameter Δ_s is greater than a critical value Δ_c, the system may order on the surface before it orders in the bulk. The system exhibits two

successive transitions, namely the surface and bulk transitions, as the temperature is lowered; Δ_c is the critical value of surface ordering at which the system orders on the surface before it orders in the bulk. If Δ_s is less than Δ_c, the system becomes ordered at the bulk transition temperature T_c^b. In the figure, we denote the paramagnetic, bulk-ferromagnetic, and surface-ferromagnetic phases by P, BF and SF, respectively, and SB denotes the multicritical point of the surface–bulk transition. The values of Δ_c, T_c^b and the surface-ordering temperature T_c^s depend on the approximate technique we use. Within the framework of the MFA, the values are respectively given by $\Delta_c = 0.25$, $k_B T_c^b / J = 6$ and

$$\frac{T_c^s}{T_c^b} = \frac{1}{24\Delta_s}(16\Delta_s^2 + 16\Delta_s + 1) \qquad \text{for} \Delta_s > \tfrac{1}{4}. \tag{7}$$

In particular, the critical value Δ_c obtained by using a variety of techniques are collected in table 2.

Table 2. The critical value of Δ_s (or Δ_c).

	MFA	Various effective-field theories	Renormalization group	Series expansion	Monte Carlo
Δ_s	0.25	0.3068 [36], 0.3297 [37] 0.4232 [38], 0.47 [39]	0.307 [40] 0.357 [40] 0.569 [41]	0.6 [42]	0.5 [43]

3.2. Surface magnetization curve

As shown in figure 3, we usually take the layered simple cubic ferromagnetic system with a (100) free surface, in which the magnetization per site on each layer is assumed to be the same. Within the framework of the MFA, the layered magnetizations of the surface, the first layer and the nth layer are given by

$$\begin{aligned} \sigma_s &= \langle S_{i\in s}^z \rangle = \tanh(4t_s\sigma_s + t\sigma_1) \\ \sigma_1 &= \langle S_{i\in 1}^z \rangle = \tanh(4t\sigma_1 + t\sigma_s + t\sigma_2) \\ \sigma_n &= \langle S_{i\in n}^z \rangle = \tanh(4t\sigma_n + t\sigma_{n-1} + t\sigma_{n+1}) \qquad \text{for } n \geq 2 \end{aligned} \tag{8}$$

with

$$t_s = \beta J_s \qquad \text{and} \qquad t = \beta J$$

where σ_{n-1} and σ_{n+1} are the magnetizations in the $(n-1)$th and $(n+1)$th layers, respectively. On the other hand, as $n \to \infty$, σ_n should approach the bulk magnetization determined by

$$\sigma_B = \tanh(6t\sigma_B). \tag{9}$$

Even within the simple framework of the MFA, we are unable to solve these coupled equations analytically. Therefore, in order to solve the coupled equations for the layered magnetizations, the following two approximations are usually used.

(i) Continuous approximation

Defining $M(R) = \langle S_i^z \rangle$ and $J_{RR'} = J_{ij'}$ from (5) the magnetization is given by

$$\sum_{R'} J_{RR'} M(R') = k_B T \tanh^{-1}(M(R)). \tag{10}$$

At this point, we treat R as a continuous variable and suppose that $M(R)$ is small in magnitude. This treatment leads (10) to the Ginzburg–Landau type equation;

$$AM(R) + BM^3(R) - C\nabla^2 M(R) = 0. \tag{11}$$

However, the existence of surface introduces an additional boundary condition

$$M_s = \lambda \left. \frac{dM}{dz} \right|_{z=0} \tag{12}$$

with

$$\lambda = \frac{a}{1 - 4\Delta_s} \tag{13}$$

where a is the lattice constant and $z = 0$ is the surface plane of the semi-infinite system, restricted to $z > 0$. Taking into account that for $z \to \infty$ M should approach the bulk magnetization M_B, equation (11) with the boundary condition (12) can be solved analytically [44, 45]. In particular, for $\lambda > 0$ (i.e. $\Delta_s < \Delta_c$), its solution gives

$$M_s \propto (T_c^b - T) \tag{14}$$

in contrast with

$$M_B \propto (T_c^b - T)^{1/2}. \tag{15}$$

Thus, the continuous approximation and its variants have been applied to the prototype, in order to study the influences of surface on the critical phenomena [2, 3]. However, the temperature dependence of M_s in the whole region below T_c^b or T_c^s could not be obtained from this approach, although it is a powerful method for investigating the critical surface properties.

(ii) Layered approximation

In order to obtain the thermal variations of surface and each layered magnetization over the whole temperature range, it is necessary to solve the coupled equations for the magnetizations, like (8) of the MFA. Although feasible, this needs a computation which requires the help of a computer. Furthermore, even if we use a numerical method, they must be terminated at a certain layer.

Figure 4(*a*) shows our result based on the effective-field theory with correlations (EFT) which is superior to the MFA [35, 46, 47]. For the case of $\Delta_s = -0.5(\Delta_s < \Delta_c)$, it is obtained by solving the coupled equations of the layered magnetizations (like (8) of the MFA) numerically until the tenth layer (or $n = 10$). The EFT can be derived by expanding the right-hand side of the exact identity (3) and by introducing the decoupling approximation

$$\langle S_j^z S_k^z \cdots S_l^z \rangle \simeq \langle S_j^z \rangle \langle S_k^z \rangle \cdots \langle S_l^z \rangle \qquad \text{for } j \neq k \neq \cdots \neq l. \tag{16}$$

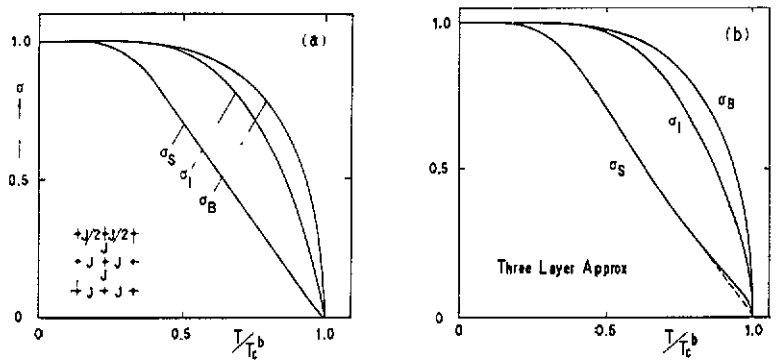

Figure 4. (*a*) Magnetization curves of the surface, first layer and bulk obtained by solving the coupled equations in the EFT until $n = 10$ numerically without introducing the layered approximation. (*b*) Magnetization curves of the surface, first layer and bulk obtained by the three-layer approximation for the same system as (*a*) [46].

into the resultant multispin correlation functions. Then the introduction of the decoupling approximation into the exact identity just corresponds to the result of Zernike approximation [48]. The bulk transition temperature T_c^b for the simple cubic lattice is given by

$$k_B T_c^b / J = 5.073. \tag{17}$$

Here, notice that the first approximation of [49] and the finite cluster expansion method [50] are also equivalent to the EFT.

Now, to solve the coupled equations for a large number of n (for instance, $n = 10$) needs great labour and also time for the computation. The simplest method for solving them is to assume that the layered magnetizations remain unaltered after a certain layer, such as $\sigma_2 = \sigma_3 = \cdots = \sigma_n = \sigma_B$, which may be termed the three-layer approximation. The EFT result for the three-layer approximation with the same situation as figure 4(*a*) is shown in figure 4(*b*). Comparing (*a*) and (*b*), the result of the three-layer approximation deviates a little from the linear behaviour (broken line) very near the bulk transition temperature, although as a whole the temperature dependences of σ_s are very similar to each other. The magnetization curve σ_s in figure 4(*a*) changes linearly with T, which is also consistent with the result of (14). Experimentally, such a linear temperature dependence of σ_s has been observed in many semi-infinite crystalline magnets [4].

Thus, the layered approximation gives a reasonable result for the thermal behaviour of σ_s except for the temperature region very near $T = T_c^b$ (or $T = T_c^s$). We can use the approximate method, in order to obtain the temperature dependence of surface magnetization as a whole. At this point, one should notice that a slight deviation from the linear behaviour (broken line) is obtained in figure 4(*b*) for the three-layer approximation. However, the region of the deviation very near $T = T_c^b$ becomes narrower when we take a better layer approximation. In other words, for the system with $\Delta_s < \Delta_c$, the surface, near $T = T_c^b$, is magnetized only by the spontaneous magnetization of the bulk, which is to be taken as far apart as the bulk correlation length from the surface [51].

An important fact should be mentioned here; the authors in [52] raised a question that the first derivative $\partial\sigma_s/\partial T$ must be discontinuous at $T = T_c^b$, when $\Delta_s > \Delta_c$, although the question was originally raised in [53]. Their arguments are based on the renormalization group method with the two-layer approximation. At the present, the argument does not seem to be definite. The first derivative of magnetization at the surface depends strongly on the boundary conditions imposed in the calculation [54–56]. In fact, the three-layer approximation for the EFT exhibits such a discontinuity, whereas for the four-layer approximation it becomes smaller. For reference, the behaviour of σ_s near $T = T_c^b$ in the MFA is depicted in figure 5, by taking the system with $\Delta_s = 0.5$ ($\Delta_s > \Delta_c$) and solving the coupled equations (8) in each layer approximation numerically. In the figure, n expresses the nth layer approximation, namely $\sigma_{n-1} = \sigma_n = \sigma_{n+1} = \cdots = \sigma_B$. On the other hand, the continuous approximation of the MFA [45] gives, for $\lambda < 0$ ($\Delta_c < \Delta_s$) and $|T_c^b - T| \ll 1$,

$$M_s(T) = M_s(T_c^b) + \frac{3|\lambda|}{aT_c^b}(T_c^b - T) + b(T_c^b - T)^2 \tag{18}$$

where $b = 0$ for $T > T_c^b$. It shows that M_s together with its first derivative is a continuous function of temperature at $T = T_c^b$, but that there is a discontinuity at $T = T_c^b$ in the second derivative of M_s.

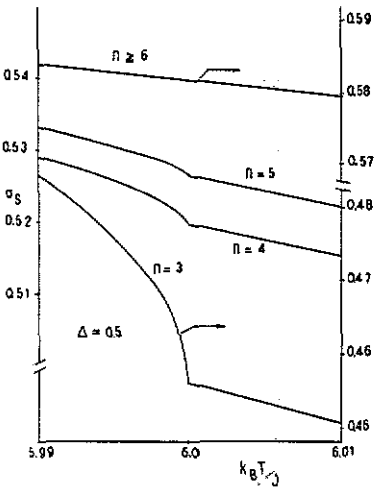

Figure 5. Temperature dependences of surface magnetization σ_s for the n-layer approximation of the prototype obtained in the MFA. The value of Δ_s is fixed at $\Delta_s = 0.5$.

Experimentally, the surface magnetization and its first temperature derivative are found to be continuous functions of temperature at $T = T_c^b$ by the electron-capture spectroscopy measurement of polycrystalline Gd [53] where T_c^s lies at least 15 K above the bulk Curie temperature $T_c^b = (292.5 \pm 0.3)$ K. Here, it is important to note that the surface magnetization of polycrystalline Gd [53, 57] is different from that of Gd(0001) on a W(110) substrate obtained by the use of spin-polarized LEED [58]. Figure 6 shows the difference between the experimental results. A characteristic feature of Gd(0001) on a W(110) substrate is the minimum at a temperature $T_{comp} \simeq 289$ K, namely a kind of compensation point. The possible explanation for the behaviour is surface

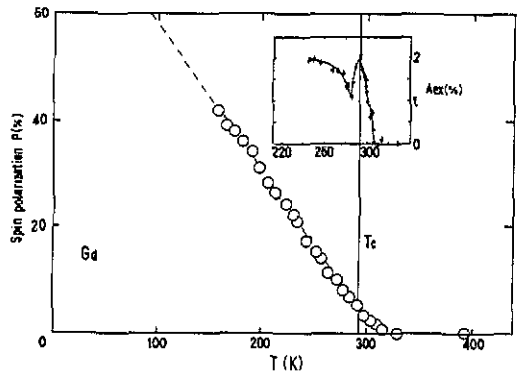

Figure 6. Surface magnetization of polycrystalline Gd film derived from the nuclear polarization of deuteron electron capture [57]. The inset is the surface magnetization (or the scattering asymmetry A_{ex}) of Gd(0001) film on W(110) obtained from spin-polarized LEED in the critical region [58].

magnetic reconstruction where the surface layer couples in an antiferromagnetic way to the rest of the system.

4. The effects of surface single-ion anisotropy

In contrast to the prototype, the research on the influence of surface single-ion anisotropy on magnetic properties at or near the surface seems to be far from a satisfactory situation, although recent experiments noted in section 2 show that there exists a very strong anisotropy field acting in the surface or at an interface. Among various models, the simplest but most useful model system including the term for single-ion anisotropy at the surface is a semi-infinite simple cubic Ising ferromagnet with a spin-1 (100) overlayer. The Hamiltonian is given by

$$H = -J_s \sum_{(ij)} S_i^z S_j^z - J \sum_{(m,n)} \mu_m^z \mu_n^z - J_1 \sum_{(i,m)} S_i^z \mu_m^z - D_s \sum_i (S_i^z)^2 \tag{19}$$

where the spin variables S_i^z take the values ± 1 and 0, μ_m^z can be ± 1, and the summations are carried out only over nearest-neighbour pairs of spins. D_s is the single-ion anisotropy parameter at the surface. Figure 7 shows a two-dimensional cross section of this system. In particular, if the surface single-ion anisotropy parameter takes an infinite positive value, this model reduces to the prototype of surface magnetism [59]. Therefore, one can compare the results obtained with the present model with those known for the prototype.

4.1. Surface tricritical behaviours

Now it is necessary to evaluate the mean values $m_s = \langle S_i^z \rangle$ and $\sigma_\nu = \langle \mu_{m\in\nu}^z \rangle$, where ν means the νth layer parallel to the (100) surface. These equations can be easily obtained by using the exact identities of the spin-1 and spin-$\frac{1}{2}$ Ising models, like the

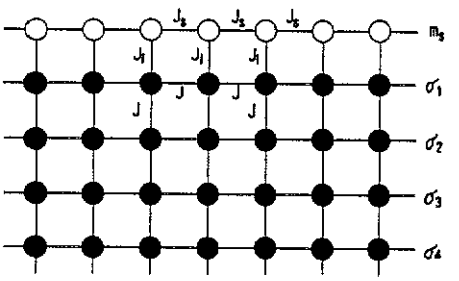

Figure 7. Part of a two-dimensional cross section through a semi-infinite Ising lattice. Full circles denote lattice points occupied by spin $\mu_m^z = \pm 1$. On the surface, lattice points are occupied by $S_i^z = \pm 1$ and 0.

prototype [47, 59–62]. In particular, if one puts $J_1 = 0$ into the present model, the surface is uncoupled to the bulk and hence it reduces to the bulk two-dimensional spin-1 Ising system of the Blume–Capel model. In this model, there exists a tricritical point at which the system changes from a second-order to a first-order phase transition, when the value of D_s becomes large and negative. In the vicinity of the second-order phase transition line, the bulk magnetization $m_b(m_b = \langle S_i^z \rangle)$ can be written as

$$m_b^2 = \frac{1 - \bar{a}}{\bar{b}} \tag{20}$$

where the bulk expressions for the parameters $\bar{a}$ and $\bar{b}$ in the EFT are given in [63]. Then, the second-order transition line is given by

$$1 = \bar{a} \qquad \text{and} \qquad \bar{b} < 0. \tag{21}$$

The right-hand side of (20) must be positive. If this is not the case, the transition is of the first order and the tricritical point can be determined from the condition

$$1 = \bar{a} \qquad \text{and} \qquad \bar{b} = 0. \tag{22}$$

When $J_1 \neq 0$, in the vicinity of the second-order phase transition line, the surface magnetization m_s of the present model (19) can be also written in the form (20), from which the surface phase diagram can be determined. A phase diagram is presented in figure 8 as a function of $|D_s|(D_s < 0)$ [59]. Open circles in the figure denote the surface tricritical point. T_c^b is then given by (17) for the EFT or $k_B T_c^b / J = 6$ for the MFA.

At this point, possible phase diagrams for a semi-infinite Blume–Capel model with a free surface are also examined within the framework of the MFA and the two-layer approximation (m_s and m_b); the system may exhibit a variety of phase transitions and multicritical points [64]. Furthermore, the phase diagrams of a semi-infinite spin-1 Blume–Emery–Griffiths model are investigated in the MFA, in order to study the surface superfluidity in mixtures of ^{3}He and ^{4}He adsorbed on graphite [65]. However, it is well known that the quadrupolar moment of each layer parallel to the surface ($q_\nu = \langle (S_i^z)^2 \rangle$ for $i \in$ the νth layer) does not appear in these works of the MFA. If one uses a more sophisticated method than the MFA, the parameters may usually

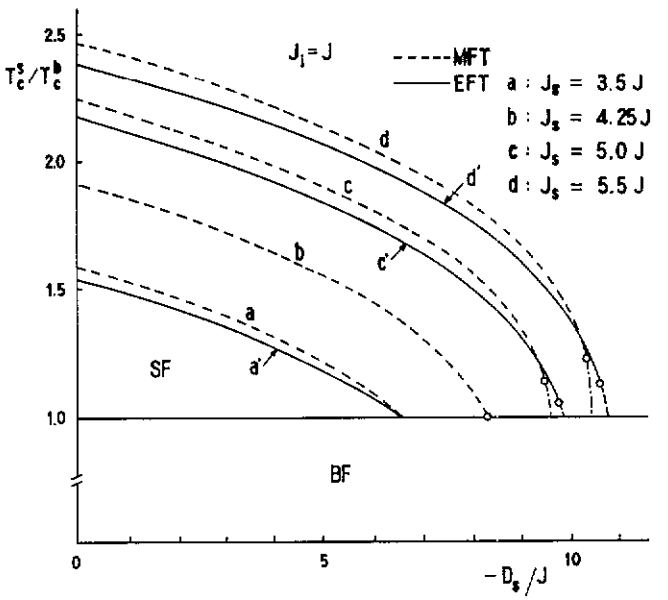

Figure 8. Surface transition temperatures of the system (19) with $J_1 = J$, plotted as a function of D_s for selected values of J_s. The curves (a)–(d) are obtained from the MFA. The curves (a'), (c') and (d') are the results of the EFT for the same values of J_s as the corresponding curves (a), (c) and (d). Open circles denote surface tricritical points. The broken curve denotes the first-order transition [59].

appear and also constitute a set of complicated coupled equations with each layer magnetization. In particular, the behaviour of q_s is in general different from those of q_ν and $q_B(q_B \equiv q_{\nu\to\infty})$, and it may play an essential role in evaluating the surface magnetization m_s (or the surface phase diagram).

As noted in section 3, it is also impossible to evaluate the coupled equations for the magnetization layer in the present model (19), even if we use a numerical method. A simple but effective method for solving them is to assume that the layered magnetizations remain unaltered after the third layer, namely the four-layer approximation $(\sigma_3 = \sigma_4 = \cdots = \sigma_n = \sigma_B)$. Here σ_B is also given by the same equation as that of the prototype. That is to say, in contrast to the models of [64, 65], it is not necessary to take account of the effects of $q_\nu(\nu \geq 1)$ on the layered magnetizations in the present model, even if we use the sophisticated technique (or the EFT) superior to the MFA. This fact greatly simplifies the treatment of the present model, like the prototype.

Let us next discuss another characteristic result for the surface tricritical behaviour which is not expected only from the phase diagram, such as figure 8. Figure 9 shows the surface magnetization curves of the present system in the EFT, when the value of $D_s/4J_s$ is taken to be -0.49 and the four-layer approximation is applied. In the bulk two-dimensional Blume–Capel model, the tricritical point exists at $D_s/4J_s = -0.47$ [66], so that if we put $J_1 = 0$, the surface magnetization should exhibit a first-order phase transition in the temperature range $0 < T < T_c^b$. In fact, the surface magnetization shows a first-order transition at $k_BT = 3.75J$ for $J_1 = 0$. By increasing the value of J_1, the gap width at the point where the surface magnetization changes discontinuously becomes smaller and finally reduces to zero when the ratio J_1/J is given by $J_1/J = 0.42$. That is to say, we find a new type of tricritical behaviour for

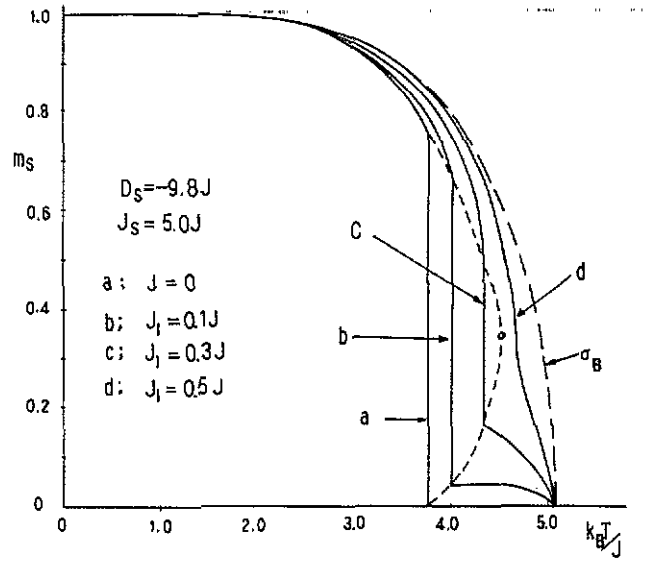

Figure 9. Temperature dependences of m_s for the system (19) with $D_s = -9.8J$ and $J_s = 5.0J$, when the value of J_1 is changed. The broken curve is the locus of the gap. The open circle is the tricritical point found for $J_1 = 0.42J$ [60].

the surface magnetization, depending on the strength of the perpendicular exchange interaction J_1. The dotted line in the figure is the locus of the gap showing the first-order transition of m_s and the open circle on the line is the tricritical point at which the first-order transition of m_s changes to the continuous transition where the gap width is reduced to zero [60]. In other words, the new type of surface tricritical behaviour depending on the strength of J_1 is also expected in the semi-infinite Blume–Capel and Blume–Emery–Griffiths models with a free surface [64, 65], although it cannot be obtained by only studying the phase diagrams.

4.2. Relation to the experimental results [I]

Experimentally, the present system (19) can be fabricated by growing a few atomic layers epitaxially on a magnetic substrate [67, 68]. The temperature dependences of the Auger polarizations from the rare earths Gd and Tb on the transition-metal surface Fe(100) and Ni(110) have been obtained recently [69]; Gd couples antiferromagnetically to both Fe and Ni, and Tb also exhibits antiferromagnetic coupling to Fe if deposited in the submonolayer range. In these systems, the magnitude of the spins on the surface is clearly different from that in the bulk.

On the other hand, the magnetic properties in the vicinity of the surface of a semi-infinite magnet can be measured by the use of the spin-polarized LEED or the Mössbauer spectroscopy. For example, depending on the energy of input polarized electrons, the spin-polarized LEED often measures the magnetic behaviour of a few layers near the surface. Therefore, it is worth investigating the total magnetization of the overlayer m_s and the first three layers of the bulk defined by

$$M = m_s + \sigma_1 + \sigma_2 + \sigma_B \tag{23}$$

where the condition $\sigma_3 = \sigma_B$ means the four-layer approximation. In the following

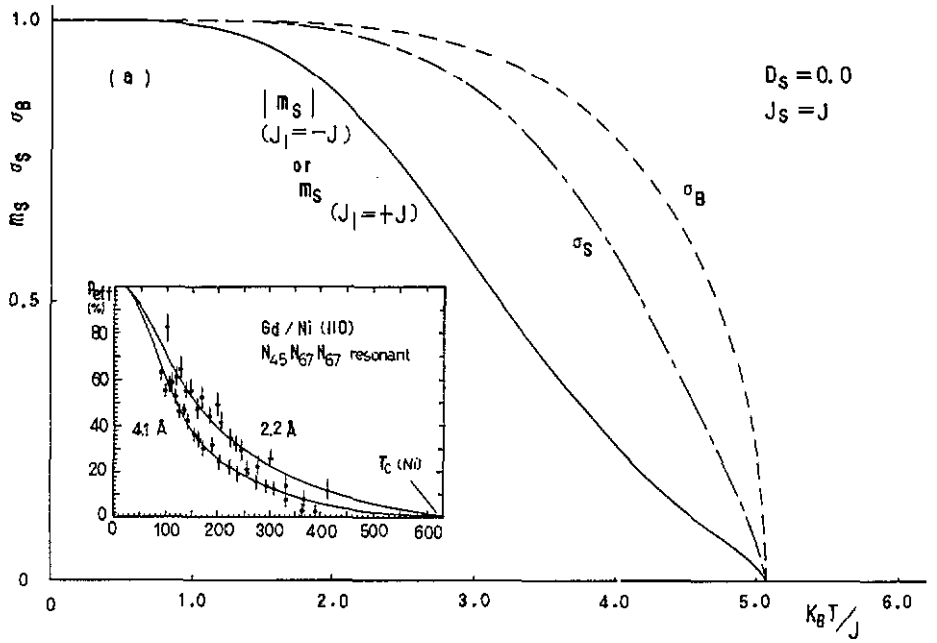

Figure 10. The temperature dependence of $|m_s|$, m_s, σ_s and σ_B for the system (19) with $D_s = 0.0$ and $J_s = J$. The inset is the experimental results of Gd on Ni(110) [61].

figures, the coupled equations of $m_s, q_s, \sigma_1, \sigma_2$ and σ_B are therefore solved numerically in the four-layer approximation of the EFT.

Figure 10 shows the numerical results, when the values of D_s and J_s are fixed at 0.0 and J respectively. In the figure, the temperature dependences of $|m_s|$ and m_s are depicted by selecting the two cases, namely $J_1 = -J$ (the surface layer is coupled antiferromagnetically to the bulk) and $J_1 = J$ (coupled ferromagnetically to the bulk). For each case, surface magnetization ($|m_s|$ or m_s) takes the same form, which exhibits a weak downward curvature. In the inset, the temperature dependences of the Auger-election spin-polarization of the resonant $N_{45}N_{67}N_{67}$ emission of two Gd films on Ni(110) are also shown, which express the weak downward curvature for the thermal variation. These results are sharply in contrast with those of the prototype. For comparison, in figure 10 the temperature dependence of the surface magnetization σ_s (chain curve) for the prototype is plotted; it can be obtained by selecting $D_s = \infty$ and $J_1 = J$ in the present system, which expresses the linear temperature dependence in the temperature region near T_c^b. The thermal variation of σ_B (broken line) is also plotted in the figure.

Notice that the m_s curves in figure 10 are obtained for $D_s = 0.0$. When the value of D_s increases to ∞, the $|m_s|$ curve gradually approaches the σ_s curve of the prototype. When the value of D_s becomes negative, the downward curvature of $|m_s|$ is more enhanced than that of $|m_s|$ for $D_s = 0.0$. As is shown in figure 2(b) of [61], the thermal variation of M for $D_s = 0.0$ shows a characteristic behaviour (a broad maximum is observed in $0 < T < T_c^b$), when the surface is coupled antiferromagnetically to the bulk. But, such a behaviour is not obtained for the surface coupled ferromagnetically to the bulk. Thus, by observing the temperature dependence of M experimentally, one may obtain a more clear distinction between the surface layer coupled antiferro-

magnetically to the bulk and the surface layer coupled ferromagnetically to the bulk (see [62] for more detail).

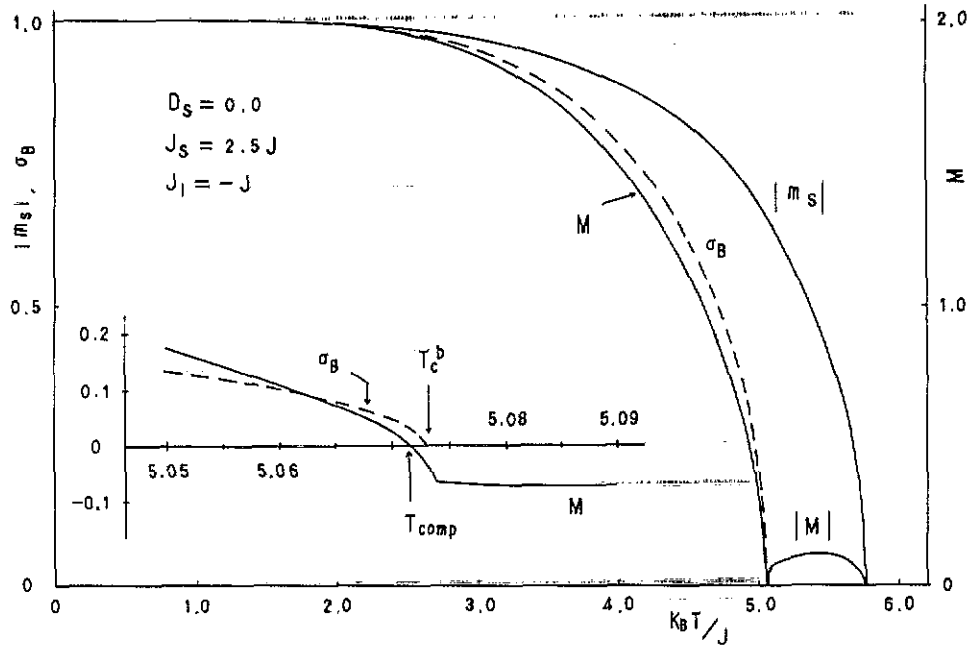

Figure 11. Temperature dependences of $|m_s|$, M and σ_B for the system (19) with $D_s = 0.0$, $J_s = 2.5J$ and $J_1 = -J$. The inset is the temperature dependences of M and σ_B in the vicinity of $T = T_c^b$ [61].

On the other hand, figure 11 shows the temperature dependences of $|m_s|$, M and σ_B (broken curve), when the values of D_s, J_s and J_1 are selected to be 0.0, $2.5J$ and $-J$ respectively. Since $J_s = 2.5J$ is larger than the critical value for surface ordering, the surface can order at the surface ordering temperature T_c^s and hence a finite surface magnetization can be obtained in the temperature region $T_c^b < T < T_c^s$. In order to clarify the behaviour of M in the vicinity of $T = T_c^b$, the inset expresses the thermal variations of M and σ_B by taking a larger scale, which clearly shows that the compensation point ($T = T_{comp}$) is obtained at a temperature a little smaller than the bulk T_c^b. At this place, it may be worth noting that a similar phenomenon ($T_{comp} < T_c^b$) is found in recent experiments for Gd and Tb films on W [58, 70] (see also figure 6), for which the surface magnetization is also coupled antiferromagnetically to the bulk.

4.3. Relation to the experimental results (II)

Depending on the surface treatments of a semi-infinite magnet, it is expected that its magnetic properties at and near the surface may exhibit large differences. In the work [71] on Gd films on W, such an example is obtained. For comparison with the inset in figure 6, the experimental results are shown in figure 12. They are similar to the experimental result [58], but some important differences can be seen; depending on the surface treatments (or a pulsed switching magnetic field of ± 4 kA m^{-1}) during cooling across the surface critical temperature T_c^s, different thermal variations of

exchange asymmetry A_{ex} (or M) are obtained by the spin-polarized LEED. In particular, figure 12(b) shows an extremely sharp structure at $T_{comp} = 290$ K, a pronounced maximum at $T_c^b = 293$ K, and falls off abruptly to zero within 2–3 K above T_c^b. T_c^s is then 296 K, which is only 3 K, but significantly, higher than T_c^b. It is proposed that the abrupt decrease in A_{ex} near T_c^s might come from the presence of a first-order magnetic surface phase transition. In figure 12(a), on the other hand, an increase in T_c^s of 17 K (from 295 to 312 K) is found by application of the field.

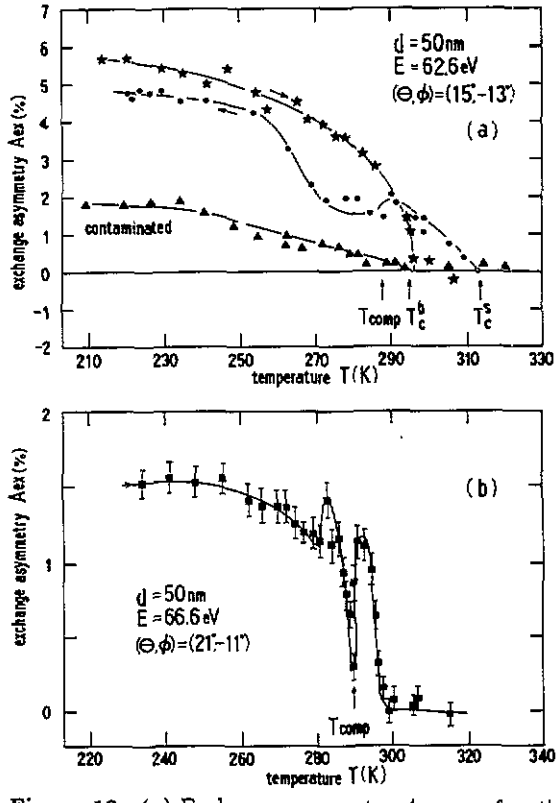

Figure 12. (a) Exchange asymmetry A_{ex} as a function of increasing temperature of a 50 nm thick clean Gd(0001) film measured after first cooling to 215 K (from epitaxy grown conditions) in the absence of an external magnetic field. Full circles represent the A_{ex} against T curve measured after subsequent cooling in a pulsed switching magnetic field of ± 4 kA m^{-1}. (b) As in (a). The sample was first cooled in the presence of a pulsed, switching magnetic field of ± 4 kA m^{-1} to 235 K. Surface magnetic order is clearly observed up to $T_c^s = 296$ K. The abrupt transition within 2–3 K at T_c^s is a direct indication of the presence of a first-order surface phase transition [71].

Now, it was proposed in [71] that these experimental results may confirm the prediction of a surface first-order transition in the theoretical works [72, 73] on the critical behaviour of a (111) free surface in a spin-$\frac{1}{2}$ FCC Ising ferromagnet. In the works based on the tetrahedron approximation of the cluster variation method, the surface transition becomes first order for a finite range of $J_s > J_{sc}$ ($J_{sc} = 1.778J$ or $\Delta_c = 0.778$). The critical points exist even for finite values of the static magnetic field and the surface transition temperature T_c^s increases in the presence of an external field.

However, these results heavily depend on the geometry of the surface (or may depend on the approximate method because the MFA does not predict the transition), since such a first-order transition is normally impossible for a spin-$\frac{1}{2}$ Ising system without a multispin interaction, such as the prototype of section 3. On the other hand, as shown in section 2.2, the easy direction of the magnetization of Gd films on W lies in the surface plane. In other words, it means that within the present system (19) the value of D_s is negative and it seems more reasonable to assume that the surface treatments of figure 12 changes the value of D_s. Furthermore, as will be discussed in the following, the surface treatments are done by a switching magnetic field, so that random magnetic fields may be induced in the surface of Gd films on W.

As was discussed in [47], these experimental results may be explained as the result of the surface tricritical behaviour in figure 8; within the present model (19), the spin-1 surface with an anisotropy constant D_s is then coupled antiferromagnetically to the bulk spin-$\frac{1}{2}$. In the bulk, Gd is assumed to be $\mu_m^z = \pm\frac{1}{2}$ with zero single-ion anisotropy. At the (100) surface, Gd ($S_i^z = \pm 1$ and 0) is assumed to take a large negative surface anisotropy. Figure 13 shows a typical result for the present system with $J_s = 5.5J$ and $J_1 = -J$, when D_s is taken to be $-10.0J$ or $-10.6J$ and the four-layer approximation is used for the numerical evaluation of the coupled equations in the EFT. In particular, the behaviour of M (or $|M|$) in the vicinity of T_c^b ($T_c^b = 5.073J$) is depicted. Then, the ratio $D_s/4J_s$ for $D_s = -10.6J$ is -0.482 and for $D_s = -10.0J$ it is -0.455. Therefore, the surface magnetization m_s can show a first-order phase transition at $T = T_c^s$ for $D_s = -10.6J$, but for $D_s = -10.0J$ it is second order. These facts can also be understood from figure 8.

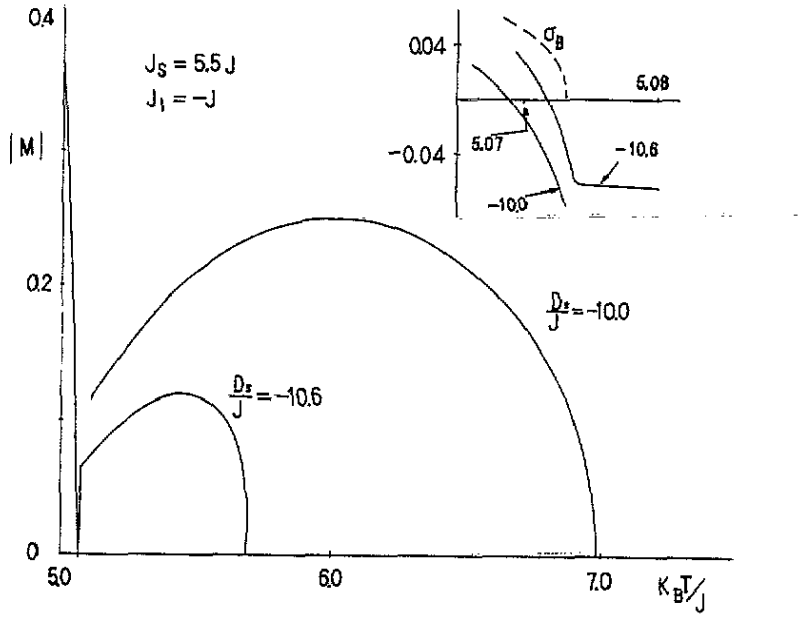

Figure 13. The thermal variations of M for the system (19) with $J_s = 5.5J$ and $J_1 = -J$ in the region near $T = T_c^b$, when the value of D_s is taken to be $-10.0J$ and $-10.6J$ (see also figure 8). Compensation points can be seen in the inset.

Comparing figure 13 with figure 12, the qualitative features in figure 13 are very similar to the experimental results in the following points:

(i) when the first-order phase transition appears, T_c^s for $D_s/J = -10.6J$ becomes less than T_c^s for $D/J = -10.0$ (or the second-order transition);

(ii) the magnitude of $|M|$ for $D_s/J = -10.6$ becomes less than that for $D_s/J = -10.0$ in the region of $T_c^b < T < T_0^s$;

(iii) T_{comp} for $D_s/J = -10.6$ is larger than that for $D_s/J = -10.0$.

In this way, these results imply that the experimental results shown in figure 12 just lie in the critical region of D_s exhibiting the surface tricritical behaviour. However, it is not clear at present whether Gd atoms on the (0001) surface have such a large negative single-ion anisotropy constant, but it may be possible for such an anisotropy to be induced by the surface treatment.

On the other hand, in order to explain the experimental data in figure 12, another interpretation may be possible. In [74], we have discussed the effects of random surface field on the surface phase diagram in a semi-infinite simple cubic spin-$\frac{1}{2}$ Ising ferromagnet with a (100) surface. The Hamiltonian is given by

$$H = -\sum_{(ij)} J_{ij} S_i^z S_j^z - \sum_i H_i S_i^z \tag{24}$$

where $S_i^z = \pm 1$ and J_{ij} takes the value J_s if both occupied spins lie on the surface and the bulk value J otherwise. H_i is the random field acting only on a site i of the surface. The probability distribution function $P(H_i)$ is given by

$$P(H_i) = \tfrac{1}{2}[\delta(H_i + H_0) + \delta(H_i - H_0)]. \tag{25}$$

The phase diagram obtained is then very similar to that of figure 8, when T_c^s is plotted as a function of H_0. We can find that the surface tricritical point exists even on the surface, when the enhanced surface interaction (6) becomes larger than $\Delta_s = 2.84$. In this way, the experimental data may be explained by the surface tricritical behaviour induced by the random surface field, just as discussed previously.

4.4. Critical phenomena

As noted before, the present model (19) reduces to the prototype, when the value of D_s is a positive infinite one ($D_s = \infty$). For the prototype, it is well known that the surface magnetization σ_s in the critical region is given by

$$\sigma_s \propto \left(1 - \frac{T}{T_c^b}\right)^{\beta_1} \qquad \text{for } \Delta_s < \Delta_c \tag{26a}$$

or

$$\sigma_s \propto \left(1 - \frac{T}{T_c^s}\right)^{\beta_1} \qquad \text{for } \Delta_s > \Delta_c \tag{26b}$$

where β_1 is a critical exponent. Within the framework of the MFA or the EFT, β_1 is given by $\beta_1 = 1$ (for $\Delta_s < \Delta_c$) or $\beta_1 = \frac{1}{2}$ (for $\Delta_s > \Delta_c$). The critical exponent β_1 for the prototype with $\Delta_s < \Delta_c$ has been studied by using various techniques and approximations [2, 3]. The theoretical results are in the range of $0.776 \leq \beta_1 \leq 0.80$. Experimentally, for instance, the mean critical exponent β_1 for both Ni(110) and Ni(001) is given by $\beta_0 = 0.8 \pm 0.2$ [75]. Another experimental result is the critical

behaviour of a semi-infinite isotropic Heisenberg ferromagnet; EuS(111) on Si(111) [76]. The surface magnetization decreases in the critical region as

$$m_s \propto \left(1 - \frac{T}{T_c^b}\right)^{\beta_1} \tag{27a}$$

with

$$\beta_1 = 0.72 \pm 0.03 \tag{27b}$$

which is clearly different from the theoretical value ($0.81 \leq \beta_1 \leq 0.88$) for the semi-infinite isotropic Heisenberg ferromagnet [75]. The result indicates the existence of a strong surface-induced anisotropy at the surface. Thus, it may be interesting to investigate the surface critical behaviour of the present model (19) as a function of D_s.

On the other hand, the critical behaviour of a semi-infinite n-vector model with an anisotropic pair interaction on the surface is examined with the use of renormalization group methods [77]. It is found that in the vicinity of T_c^s the value of β_1 corresponding to an easy magnetization axis is significantly smaller (about 38%) than that corresponding to a hard magnetization axis; for the easy direction $\beta_1 = 0.35$ is obtained. Notice that from the measurements of uncoated epitaxial films of Tb(0001) on W(110) in the neighbourhood of T_c^s, $\beta_1 = 0.348 \pm 0.01$ is obtained for the surface magnetization along the easy axis [78].

4.5. Related works

From section 4.1 to 4.4, we have mainly reviewed the effects of surface single-ion anisotropy on magnetic behaviours in a semi-infinite spin-$\frac{1}{2}$ Ising model with a spin-1 overlayer. On the other hand, the roles of surface anisotropy in a semi-infinite Heisenberg model with a free surface have been discussed very recently by the use of various methods.

Experimentally and theoretically, it is now well known that the thermal dependence of M_s at low temperatures is given by, because of the spin excitations at the surface,

$$\frac{M_s(T)}{M_s(0)} = 1 - B_s T^{3/2} \qquad B_s = \lambda_s B_b \tag{28}$$

where B_s is the proportionality factor at the surface and B_b its bulk counterpart. In the classical law [79], λ_s is given by $\lambda_s = 2$, although various measurements of real systems [7, 80] show $\lambda_s > 2$. For the thickness dependence of λ_s, for example, see the recent work [81] for epitaxial Fe(110) films on W(110) of thickness between 7 and 40 Å. In particular, the effects of surface anisotropy on the $T^{3/2}$ law and λ_s were examined in recent work [82, 83].

In [84], the possibility of spin canting near the surface of a semi-infinite Heisenberg ferromagnet with a spatially varying demagnetizing field and the surface anisotropy field H_s is examined in the continuous approximation. It is shown that the spin canting occurs only when the value of H_s exceeds a critical value which is large compared with surface anisotropy fields inferred from experiments [20]. At this point, if the surface spins are oriented out of the surface, this generates magnetic stray fields and, in order to minimize the magnetic stray field energy, the spin configuration near the surface

is expected to relax to some new configuration at and near the surface. In this work, however, such an effect of stray field is not taken into account for the estimation of the critical field.

On the other hand, the influences of $D_s(D_s > 0)$ on the Curie temperature and spontaneous magnetization of each atomic plane in the thin film thickness l ranging from $l = 1$ to $l = 17$ are examined on the basis of the simple cubic Heisenberg model with (100) planes [85]. For a strong surface anisotropy ($D_s = J$) the Curie temperature rises as l is decreased, and conversely for a weak anisotropy ($D_s = 0.01J$) it decreases from the value at the middle plane and reaches a minimum at the surface plane. There seems to be a critical value $D_s^*(D_s^* > 0)$ where $T_c^{-1}\mathrm{d}T_c/\mathrm{d}l$ tends to be positive when $D_s < D_s^*$ and negative when $D_s > D_s^*$. Unfortunately, the critical value D_s^*, the possibility of surface tricritical behaviour (or for $D_s < 0$) and the effects of D_s and l on the $T^{3/2}$ law and λ_s are not investigated. In [86], the AC magnetic susceptibility of a Gd(0001) film with film thickness about 42 atomic layers on a W(110) substrate is measured and it shows a rapid drop within 4 K from the Hopkinson maximum. This result may also characterize the first-order character of the surface phase transition. However, this measurement probes the whole volume of the Gd(0001) thin film, so that it provides information about the average properties of the sample. At the present, it is not clear whether it results from the surface tricritical behaviour or from the perpendicular interaction J_1, discussed in this section.

5. Random anisotropy at surface or interface

In amorphous rare earth–transition metal and rare earth alloys, it is well known that the crystal-field Hamiltonian H_c can be written as

$$H_c = -\bar{D}\sum_i (S_{z_i})^2 \tag{29}$$

where the local easy axis z_i at each site is randomly distributed in direction and the value of $\bar{D}$ is positive. This random anisotropy model (RAM) has probably been a good description of the microscopic magnetism in the bulk for these materials [87].

On the other hand, the surfaces of crystalline ferromagnets are sometimes subjected to inhomogeneities not found in the bulk. This is so because crystals are grown on substrates, and at the interface there can be lattice mismatches, interdiffusions of atomic species, etc. In order to understand the experiments on single-crystal Fe films grown on GaAs, a model has recently been proposed [88], in which the axes of single-ion anisotropy are randomly distributed over a surface region of the crystalline ferromagnet. In other words, a thin layer of amorphous magnetic material on a single crystal of Fe (or a kind of surface amorphization of a semi-infinite crystalline ferromagnet [89]) is considered. The layer is taken to be described by ferromagnetic exchange and a random uniaxial anisotropy, with a thickness z_0 (see figure 14(a)). Upon including the exchange interaction term the Hamiltonian density is given by

$$H = \tfrac{1}{2}A(\nabla\Phi)^2 - \bar{D}(z)\cos^2(\Phi - \eta(r)) \qquad z > 0 \tag{30}$$

where $\bar{D}(z) = \bar{D}$ for $z < z_0$ and $\bar{D}(z) = 0$ for $z > z_0$. Φ is the angle that the magnetization vector makes with respect to an arbitrarily chosen axis in the xy plane.

η is a random function of the position vector. The averaged magnetization in the $z > z_0$ region is then given by

$$M(Z) = M_0 \left(1 - \frac{\lambda}{\alpha z} e^{-\alpha z}\right) \tag{31}$$

with

$$\alpha = (K/A)^{1/2} \qquad \text{and} \qquad \lambda = \frac{\Omega z \bar{D}^2}{32\pi^2 \bar{A}^2} \tag{32}$$

where K is the bulk crystalline anisotropy density and Ω the volume over which the random axes are correlated. From this argument, the authors in [88] found that the random anisotropy in the interface layer induces weakly pinned fluctuations of the magnetization which penetrate approximately to 100 Å, in accordance with magnetization measurements of Fe on GaAs [90].

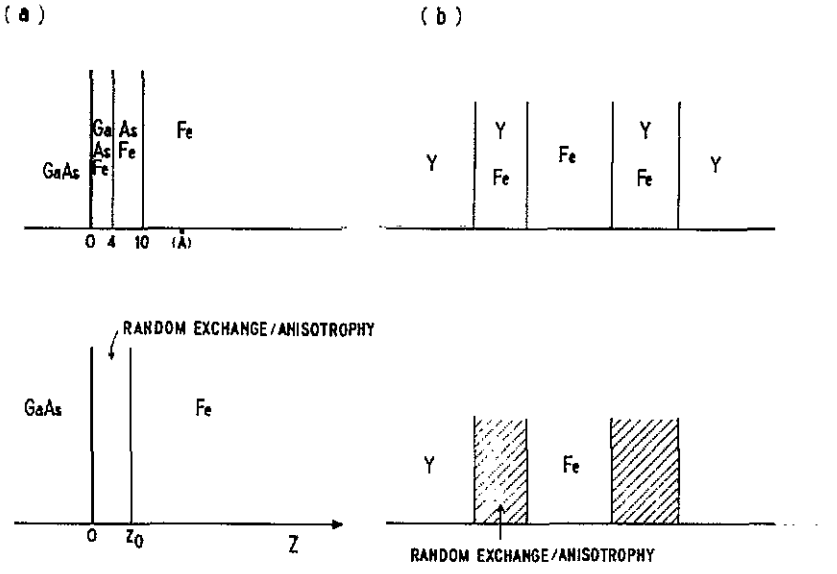

Figure 14. Schematic pictures on which the models of section 5 are based.

At this point, there exist other experiments which may indicate the validity of the large RAM near the surface [91a–b]. The surface magnetization of amorphous $Fe_{78}B_{13}Si_9$ alloy (Metglas 2605S2) is probed using neutron reflectometry. The magnetic moment as a function of depth z into the ribbon is found to be consistent with an exponential variation of the form

$$\delta\mu(z) = \delta\mu_s \exp(-z/\xi) \tag{33}$$

where $\delta\mu(z)$ is the difference between the moment value at a depth z and that in the bulk, $\delta\mu_s$ is the difference between the moment value in the bulk and at the surface, and ξ is a magnetic coherence length. The values obtained experimentally are then $\delta\mu_s = 10.3\mu_B$ and $\xi = 81$ Å. The coherent length is clearly different from that of the

prototype in section 3, where it is typically of atomic distances, $\xi \sim 2$ Å [92]. The data are explained by invoking a spread in moment directions ($\simeq \pm 50°$) at the sample surface, penetrating some 40 nm into the bulk and the moment canting at the surface is interpreted in terms of the effect of fine scale surface roughness. In other words, the surface roughness may induce the large random anisotropy at each Fe site of the surface. For more information about the surface anisotropy of the amorphous ribbons see [93]; it is proposed that there exists another (unknown) anisotropy constant K_a other than the surface shape and stress-induced anisotropies. It may be the random anisotropy at the surface.

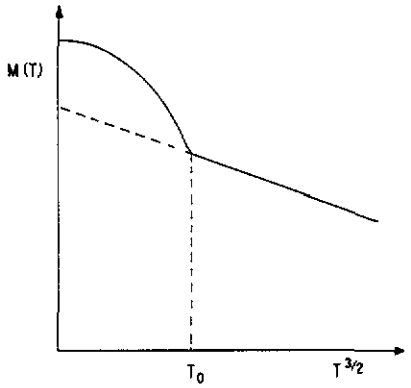

Figure 15. The temperature dependence of magnetization for an asperomagnetic system. T_0 is a characteristic temperature at which the system dissolves completely into microdomains.

Now, the present author has considered [94, 47] that the temperature dependence of magnetization at low temperatures in an asperomagnet (due to the RAM with $\bar{D} < \bar{J}$, $\bar{J}$ = mean interaction randomly averaged) may be expected to be similar to that in figure 15. In the figure, T_0 corresponds to the temperature at which the system dissolves completely into microdomains and below which the $T^{3/2}$ law becomes ill defined; there exist finite ferromagnetically ordered magnetic regions (microdomains) with small effective uniaxial anisotropies. However, the easy axes of different regions are ordered at random and the effective spins of microdomains are distributed at random in a cone with half angle ϕ. Experimentally, such a marked deviation from the $T^{3/2}$ law at low temperatures has recently been observed for magnetic excitations of amorphous Sm–Ni thin films in an applied field ($H \simeq 10$ kOe) [95]. There is a temperature T_0 below which the Sm ion random anisotropy $\bar{D}$ is very strong and ϕ is relatively large, and therefore the magnetic excitations are suppressed. Here, notice that a finite magnetic field is applied in the measurement.

In the RAM with $\bar{D} < \bar{J}$, three different magnetic structures are theoretically predicted, according to the strength of the external magnetic field [96, 97]. In a low-field regime the system is in a correlated speromagnetic phase, where spin excitations may not be observed [87]. But, in a second, high-field regime, a new phase with a wandering axis is produced. This phase may exhibit a slightly non-collinear spin structure in which the tipping of the magnetization with respect to the external field varies over the sample. In other words, it is a field-induced asperomagnetic phase. As discussed previously, spin excitations can be observed here. In the third, high-field regime, the non-collinear spin structure closes even further toward the field.

In relation to this discussion, the following observations should be noted; very recently the spin-wave excitations of compositionally modulated thin films of Y/Fe [98] have been measured in the applied field $H = 50$ kOe and a marked deviation from the $T^{3/2}$ law is observed below 30 K, like the spin-wave excitations of amorphous Sm–Ni thin film. Comparing the case of Fe films on GaAs with this experiment, the origin of random anisotropy is very similar. The situation is also depicted in figure 14(b). Some diffusion of Y into Fe occurs and this creates amorphous Fe–Y layers at the interface, like the amorphous bulk Fe–Y alloy [99] where an asperomagnetic spin structure is observed for a high Fe concentration. Then, the source of the random anisotropy in the region may be the polarization of the Fe layers by the diffused Y atoms and the surface roughness. In other words, if the random anisotropy model is valid for the interface region of Fe films on GaAs, a marked deviation from the $T^{3/2}$ law would be found at low temperatures by making a multilayered Fe–GaAs sample similar to the multilayered Fe–Y samples, although such an observation has not yet been reported.

In summary we have developed only a few aspects of surface magnetism, paying attention to the various effects of anisotropy at the surface to the magnetic properties. Much progress is awaited in the next few years where new experimental techniques as well as theoretical work may provide important information.

Acknowledgments

This work is based on my talks given at the fifth ICPMM held at Madralin, October 1990 [47]. The author wishes to acknowledge Dr M R J Gibbs (University of Bath), Professors H Szymczak and H K Lachowicz (Institute of Physics, Warsaw) for their interest in the talks.

References

[1] Mills D K 1971 *Phys. Rev.* B 3 3887
[2] Binder K 1983 *Phase Transitions and Critical Phenomena* vol 8, ed C Domb and J L Lebowitz (London: Academic) p 1
[3] Diehl H W 1986 *Phase Transitions and Critical Phenomena* vol 10, ed C Domb and J L Lebowitz (London: Academic) p 76
[4] Kaneyoshi T 1991 *Introduction to Surface Magnetism* (Boca Raton, FL: CRC Press)
[5] Dewames R E and Wolfram T 1972 *Progress in Surface Sciences* vol 2, ed S G Davison (Oxford: Pergamon) p 23
[6] Mills D L 1984 *Surface Excitations* ed V M Agranovich and R Loudon (Amsterdam: Elsevier) ch 3
[7] Siegman H C, Mauri D, Scholl D and Kay E 1988 *J. Physique Coll.* C8 8
[8] Cottam M G and Tilley D R 1989 *Introduction to Surface and Superlattice Excitations* (Cambridge: Cambridge University Press)
[9] Mathon J 1988 *Rep. Prog. Phys.* 51 1
[10] Hasegawa H 1990 *Magnetic Properties of Low-dimensional Systems II* ed L M Falicov, F Mejia-Lira and J Morán-López (Berlin: Springer) p 175
[11] Freeman A J, Fu C L, Shnishi S and Weinert M 1985 *Polarized Electrons in Surface Physics* ed R Feder (Singapore: World Scientific) p 3
[12] Freeman A J, Fu C L, Lee J I and Oguchi T 1987 *Physics of Magnetic Materials* ed M Takahashi *et al* (Singapore: World Scientific)
[13] Chun L I, Freeman A J and Fu C L 1990 *J. Magn. Magn. Mater.* 83 51
[14] Rau C, Jin C and Xing G 1990 *Phys. Lett.* **144A** 406
[15] Lieberman L N, Fredkin D R and Shore H B 1969 *Phys. Rev. Lett.* 22 539

[16] Néel L 1954 *J. Phys. Radium* **15** 225
[17] Gradmann U 1986 *J. Magn. Magn. Mater.* **54–57** 733
[18] Heinrich B, Urquhart K B, Arrott A S, Cochran J F, Myrtle K and Purcell S T 1987 *Phys. Rev. Lett.* **59** 1756
[19] Koon N C, Jonker B T, Volkening F A, Kreb J J and Prinz G A 1987 *Phys. Rev. Lett.* **59** 2463
[20] Purcell S T, Heinrich B and Arrott A S 1988 *J. Appl. Phys.* **64** 5337
Dutscher J R, Cochran J F, Heinrich B and Arrott A S 1988 *J. Appl. Phys.* **64** 6095
[21] Pescia D, Stampanoni M, Bona G L, Voterlaus A, Williams R F and Meier F 1987 *Phys. Rev. Lett.* **58** 2126
[22] Jonker B T, Walker K H, Kisher E, Prinz G A and Carbone C 1986 *Phys. Rev. Lett.* **57** 142
[23] Pierce D T 1987 *Surf. Sci.* **189–190** 710
[24] Liu C and Bader S D 1990 *Magnetic Properties of Low-dimensional Systems* ed L M Falicov, F Mejia-Lira and J L Morán-López (Berlin: Springer) p 22
[25] Pappas D P, Kämper K P and Hopster H 1990 *Phys. Rev. Lett.* **64** 3179
[26] Gay J G and Richter R 1986 *Phys. Rev. Lett.* **56** 2728
[27] Karas W, Noffke J and Fritsche L 1989 *J. Chem. Phys. Phys. Chem. Biol.* **86** 861
[28] Li C, Freeman A J and Fu C L 1990 *J. Magn. Magn. Mater.* **83** 51
[29] Gay J G and Richter R 1987 *J. Appl. Phys.* **61** 3362
[30] Berghaus A, Farle M, Li Y and Banberschke K 1990 *Magnetic Properties of Low-dimensional Systems II* ed L M Falicov, F Mejia-Lira and J L Morán-López (Berlin: Springer) p 61
[31] Korecki J and Gradmann U 1985 *Phys. Rev. Lett.* **55** 2491
[32] Oepen H P and Kirschner J 1989 *Phys. Rev. Lett.* **62** 819
[33] Scheinfein M R, Unguris J, Celotta R J and Pierce D T 1989 *Phys. Rev. Lett.* **63** 668
[34] Scheinfein M R, Unguris J, Celotta R J and Pierce D T 1990 *Magnetic Properties of Low-dimensional Systems II* ed L M Falicov, F Mejia-Lira and J L Morán-López (Berlin: Springer) p 2
[35] Callen H B 1963 *Phys. Lett.* **4** 161
[36] Kaneyoshi T, Tamura I and Sarmento E F 1983 *Phys. Rev.* B **28** 6491
[37] Tamura I, Sarmento E F, Fittipaldi I P and Kaneyoshi T 1983 *Phys. Status Solidi* (b) **118** 409
[38] Sarmento E F, Tamura I and Kaneyoshi T (1984) *Z. Phys.* B **54** 241
[39] Sanchez J M and Morán-López J L 1986 *Magnetic Properties of Low-dimensional Systems* ed L M Falicov and J L Morán-López (Berlin: Springer) p 114
[40] Burkhard T W and Eisenmiegler E 1977 *Phys. Rev.* B **16** 3213
[41] Tsallis C 1986 *Magnetic Properties of Low-dimensional Systems* ed L M Falicov and J L Morán-López (Berlin: Springer) p 98
[42] Binder K and Hohenberg P C 1974 *Phys. Rev.* B **9** 2194
[43] Binder K and Landau D P 1984 *Phys. Rev. Lett.* **52** 318
[44] Kumar P 1974 *Phys. Rev.* B **10** 2928
[45] Lubensky T C and Rubin M H 1975 *Phys. Rev.* B **12** 3885
[46] Kaneyoshi T 1988 *Rev. Solid State Sci.* **2** 39
[47] Kaneyoshi T 1991 *Physics of Magnetic Materials* (Proceedings of the 5th ICPMM, Madralin, Poland, 1990) (Singapore: World Scientific) to be published
[48] Zernike F 1940 *Physica* **7** 565
[49] Matsudaira N 1973 *J. Phys. Soc. Japan* **35** 1593
[50] Benyoussef A, Boccara N and Saber M 1985 *J. Phys. C: Solid State Phys.* C **18** 4275
[51] Wolfram T, Dewames R E, Hall W F and Palmberg P W 1974 *Surf. Sci.* **28** 45
[52] Tsallis C and Chame A 1988 *J. Physique Coll.* C8 1619
[53] Rau C and Robert M 1987 *Phys. Rev. Lett.* **58** 2714
[54] Morán-López J L and Sanchez J M 1989 *Phys. Rev.* B **39** 9746
[55] Payandeh B and Robert M 1990 *Phys. Rev.* B **41** 2339
[56] Landau D P and Binder K 1990 *Phys. Rev.* B **41** 4786
[57] Rau C 1982 *J. Magn. Magn. Mater.* **30** 141
[58] Weller D, Alvarado S F, Gudat W, Schröder K and Campagna M 1985 *Phys. Rev. Lett.* **54** 1555
[59] Sarmento E F and Kaneyoshi T 1988 *Rev. Bras. Fis.* **18** 356
[60] Kaneyoshi T 1990 *Physica* A **163** 533
[61] Kaneyoshi T 1990 *J. Magn. Magn. Mater.* **89** L1
[62] Kaneyoshi T 1991 *Phys. Rev.* B **43** 6109

[63] Kaneyoshi T 1986 *J. Phys. C: Solid State Phys.* 19 L557
[64] Benyoussef A, Boccara N and Saber M 1986 *J. Phys. C: Solid State Phys.* 19 1983
[65] Jiang X P and Giri M R 1988 *J. Phys. C: Solid State Phys.* 21 995
[66] Siqueira A F and Fittipaldi I P 1986 *Physica* A 138 592
[67] Taborelli M, Allenspach R, Boffa G and Landolt M 1986 *Phys. Rev. Lett.* 56 2869
[68] Carbone C and Kisker E 1987 *Phys. Rev.* B 36 1280
[69] Paul O, Toscano S, Hüfrsh W and Landolt M 1990 *J. Magn. Magn. Mater.* 84 L7
[70] Rau C, Jin C and Robert M 1989 *Phys. Lett.* 138A 334
[71] Weller D and Alvarado S F 1988 *Phys. Rev.* B 37 9911
[72] Sanchez J M and Morán-López J L 1987 *Phys. Rev. Lett.* 58 1120
[73] Sanchez J M and Morán-López J L 1988 *Surf. Sci.* 198 L299
[74] Kaneyoshi T and Li Z Y 1989 *Physica* A 155 116
[75] Alvarado S F, Campagna M, Ciccacci F and Hopster H 1982 *J. Appl. Phys.* 53 7920
[76] Dauth B H, Alvarado S F and Campagna M 1987 *Phys. Rev. Lett.* 58 2118
[77] Diehl H W and Eisenriegler E 1984 *Phys. Rev.* B 30 300
[78] Rau C, Jin C and Robert M 1989 *Phys. Lett.* 138A 334
[79] Rado G T 1957 *Bull. Am. Phys. Soc.* 2 127
Mills D L and Maradudin A A 1967 *J. Phys. Chem. Solids* 28 1855
[80] Walker J C, Droste R, Stern G and Tyson J 1984 *J. Appl. Phys.* 55 2500
[81] Korecki J, Przybylski M and Gradmann U 1990 *J. Magn. Magn. Mater.* 89 325
[82] Mills D L 1989 *Phys. Rev.* B 40 11153
[83] Pini M G and Rettori A 1990 *Phys. Rev.* 41 779
[84] Mills D L 1989 *Phys. Rev.* B 39 12306
[85] Shi Long-Pei 1987 *J. Appl. Phys.* 61 4267
[86] Salas F H 1990 unpublished work
Salas F H and Mirabal-Garcia M 1989 *J. Appl. Phys.* 66 5523; 1990 *Phys. Rev.* B 41 10859
[87] Kaneyoshi T 1984 *Amorphous Magnetism* (Boca Raton, FL: CRC)
[88] Cullen J R, Hathaway K B and Coey J M D (1988) *J. Appl. Phys.* 63 3649
Cullen J R 1988 *J. Magn. Magn. Mater.* 73 167
[89] Kaneyoshi T 1989 *Phys. Rev.* B 39 557
[90] Schröder K, Prinz G A, Walker K H and Kisher E 1985 *J. Appl. Phys.* 57 3669
[91a] Ivison P K, Cowlam N, Gibbs M R J, Penfold J and Shackleton C 1989 *J. Phys.: Condens. Matter* 1 3655
[91b] Ivison P K, Cowlam N, Zhuping Zhong and Williams J M 1990 *J. Non-Crystall. Solids* 117–18 666
[92] Alvarado S F 1979 *Z. Phys.* B 33 51
[93] Ding B Z, Lu J, Wang J T, Li S L and Li G S 1990 *J. Magn. Magn. Mater.* 89 70
[94] Kaneyoshi T 1985 *Int. Symp. on Magnetism of Amorphous Materials, Balatonszeplak, Hungary (October, 1985)* plenary talk; Kaneyoshi T and Li Z Y 1987 *Prog. Phys.* 7 264 (in Chinese)
[95] Peng C B, Dai D S, Fang R Y and Liu Z Y 1989 *J. Magn. Magn. Mater.* 79 11
[96] Chudnovsky E M and Serota R A 1983 *J. Phys. C: Solid State Phys.* 16 4181
[97] Chudnovsky E M, Saslow W M and Serota R A 1986 *Phys. Rev.* B 33 251
[98] Badia F, Ferrater C, Lousa A, Martinez B, Labarta A and Tejada J 1990 *J. Appl. Phys.* 67 5652
[99] Chappert J, Coey J M D, Liénard A and Rebouillat J P 1981 *J. Phys. F: Met. Phys.* 11 2727